

## Anti-phase boundaries and phase transitions in titanite: An X-ray diffraction study

JUTTA CHROSCH,<sup>1</sup> ULRICH BISMAYER,<sup>2</sup> AND EKHARD K.H. SALJE<sup>1</sup>

<sup>1</sup>Department of Earth Sciences, University of Cambridge, Downing Street, Cambridge CB2 3EQ, U.K.

<sup>2</sup>Mineralogisch-Petrographisches Institut, Universität Hamburg, Grindelallee, D-20146 Hamburg, and SFB 173, Universität Hannover, Germany

### ABSTRACT

X-ray diffraction rocking curves of titanite, CaTiSiO<sub>5</sub>, were measured using a novel high-resolution diffractometer. Three Bragg reflections were recorded as a function of temperature and their profiles analyzed in terms of a Gaussian Bragg peak and a diffuse scattering component with an overall Lorentzian shape. The temperature dependence of the Gaussian intensities of the rocking peaks of superstructure reflections, *hkl* with *k* + *l* odd, scale with the long-range order parameter as  $I \propto Q^2 \propto |T - T_c|^{2\beta}$ , where  $\beta = 0.14(1)$  is the effective order parameter exponent.

The diffuse scattering intensity changes little with temperature at  $T < T_c - 20$  K. Strong diffuse scattering is found at  $T > T_c$  with centers of their Lorentzian diffraction profiles shifted by  $\Delta\omega \approx 0.5^\circ$  with respect to the position of the equivalent Bragg peak. A second phase transition at 825 K is confirmed and the possibility of a third transition at  $\sim 1150$  K is discussed.

### INTRODUCTION

The reversible structural phase transition at  $\sim 500$  K in synthetic titanite, CaTiSiO<sub>5</sub>, (Taylor and Brown 1976) appears to generate remarkably thick and mobile anti-phase boundaries (APBs) at  $T \approx T_c$  (Speer and Gibbs 1976; Van Heurck et al. 1991). Van Heurck et al. (1991) also observed that a synthetic crystal was riddled with APBs at room temperature. We repeated electron microscopic observations on a very pure, synthetic crystal that was previously investigated by Bismayer et al. (1992), Salje et al. (1993), and Kek et al. (1994) and found that this crystal contained only very few APBs at room temperature. Because this titanite crystal showed clearly pronounced phase transitions at 496 and 825 K (Salje et al. 1993; Zhang et al. 1995, 1996; Meyer et al. 1996) the appearance APBs is clearly not a prerequisite of the transition mechanism. The APBs may, however, modify the transition behavior so that natural samples with many impurities may contain many APBs and may not display the truly intrinsic transition mechanism as observed in synthetic samples of high purity.

In this study we were concerned only with clean material for identification of the intrinsic thermodynamic behavior of titanite. Previous investigations on such crystals (Bismayer et al. 1992; Kek et al. 1994) identified the same basic structural changes from an averaged  $A2/a$  structure to the low-temperature  $P2_1/a$  phase that can be described by shifts of the Ti atoms from the centers of the TiO<sub>6</sub> octahedra forming anti-parallel aligned chains in the low-symmetry phase as discussed by Taylor and Brown (1976). Previous X-ray diffraction experiments showed that the Bragg reflections *hkl* with *k* + *l* odd show

a temperature dependence that could be fitted with an empirical power law  $I \propto Q^2 \propto |T - T_c|^{2\beta}$  with  $\beta = 0.15$  (Bismayer et al. 1992; Schmidt et al. 1993). The intensity, *I*, in these experiments included diffuse scattering, which does not reflect the long-range order parameter but relates to lattice imperfections such as APBs and point defects. Depending on the amount of diffuse scattering the reflection profile can be Gaussian, Lorentzian, or a combination of both. To explore the temperature dependence of the long-range order independently of the effect of lattice imperfections we measured X-ray rocking curves on reflections  $\bar{2}16$  and  $\bar{1}43$ , as well as on the non-superstructure reflection  $\bar{1}42$ . By separating Gaussian and Lorentzian diffraction signals the effective order-parameter exponent is correlated with the thermodynamic characteristics of the phase transition(s) in titanite.

We argue in this paper that the diffuse diffraction intensities (and hence the lattice imperfections) do not change at temperatures below  $T_c - 20$  K despite the strong temperature dependence of the long-range order parameter. Furthermore, the long-range order parameter shows a “clean” phase transition with no detectable defect fields that would be visible at temperatures above the transition point.

### EXPERIMENTAL METHOD

#### Diffraction geometry

In this study we used a high-resolution diffractometric method, which was successfully applied to the determination of ferroelastic twin-wall widths (Wruck et al. 1994; Chrosch and Salje 1994; Salje and Chrosch 1996; Chrosch and Salje 1996; Locherer et al. 1996). In our

instrument a highly monochromatic  $\text{CuK}\alpha_1$  beam with a diameter of  $\sim 100 \mu\text{m}$  is focused on the surface of the sample. The diffracted intensity is measured using either a  $120^\circ$  ( $2\theta$ ) position-sensitive detector, where the distance between two channels is equal to  $\Delta(2\theta) = 0.028^\circ$ , or an area detector with similar resolution. The distance between the specimen and the detectors can be varied and were chosen to be 300 and 240 mm, respectively, for the two detectors. The experimental flexibility of the instruments is further enhanced by six possible independent movements of the sample in the beam: two tilts ( $\omega$ ,  $\chi$ ), two perpendicular translations, a rotation of the sample ( $\Phi$ ), and an out-of-plane movement of the detector ( $Y$ ) (Salje 1995).

To measure the temperature dependence of the rocking-profile the sample holder consisted of a ceramic furnace with a relative temperature stability of  $\pm 0.5 \text{ K}$  as determined with a chromel-alumel thermocouple within the furnace and  $\sim 1 \text{ mm}$  from the bottom of the sample. The single crystal of titanite with a size of  $3 \times 3 \times 4 \text{ mm}$  was mounted on the furnace with silver paste and adjusted at room temperature to optimize the diffraction signals. For reflection  $\bar{2}16$  the diffraction angle is  $2\theta = 91.0^\circ$ , and with the angle  $\Psi$  between (001) and  $(\bar{2}16)$  equal to  $17.7^\circ$  the corresponding tilt in  $\omega$  was  $27.8^\circ$ . In that optimum position the tilt axis lies parallel to the crystallographic  $[1\bar{2}0]$  direction.

In a first set of experiments rocking curves were recorded at room temperature within a rotation range ( $\Delta\Phi$ ) of  $\pm 3^\circ$  (step size  $0.2^\circ$ ) and a tilt interval of  $\pm 2^\circ$  ( $\Delta\omega$ , step  $0.01^\circ$ ) around the reflection counting each step for 60 s. The temperature dependent measurements were started at  $T = 365 \text{ K}$  and temperature was increased to 510 K using similar angular parameters and times per setting. The integrated intensities were determined by least-squares fits of the counts in the various channels to a Gaussian function. Rocking curves and integral  $2\theta$  curves were constructed as described below.

In a second set of experiments rocking curves for reflections  $\bar{1}42$  and  $\bar{1}43$  were recorded simultaneously using an area detector. A small piece was cut from the original titanite crystal and mounted on top of a fiber located within a horseshoe furnace. The temperature stability of that arrangement was of the order of  $\pm 1 \text{ K}$  and was calibrated using a chromel-alumel thermocouple at the position of the crystal. With the relevant diffraction angles  $2\theta = 50.2^\circ$  ( $\bar{1}42$ ) and  $59.9^\circ$  ( $\bar{1}43$ ) and  $\omega \approx 39.6^\circ$  (for both reflections, the following instrument parameters were used:  $38.5 \leq \omega \leq 41.0^\circ$  (step  $0.02^\circ$ ,  $t = 300 \text{ s}$  per step),  $35 \leq 2\theta \leq 75^\circ$ , and  $70 \leq \chi \leq 110^\circ$  (for definition of angles see Salje 1995). The temperature was increased from 295 to 1100 K in steps of nominally 50 K. Three different rocking curves were calculated by integration over  $\omega$ ,  $2\theta$ , and  $\chi$ , respectively. In addition, two- and three-dimensional maps of reciprocal space were calculated for every temperature and each of the reflections.

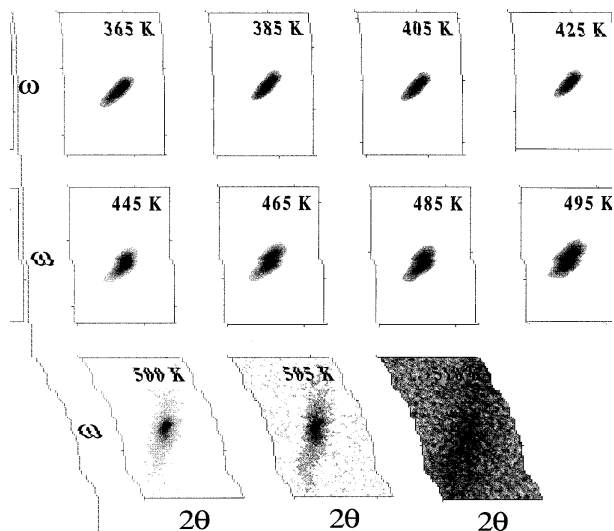


FIGURE 1. A series of diffraction profiles in the  $\omega$ - $2\theta$  plane at various temperatures. The reflection is  $\bar{2}16$ ; the direction of the elongation is  $[2\bar{1}6]^*$ . At temperatures below  $T_c$  its width of  $\sim 2.5 \text{ mrad}$  yields a domain size of  $1000 \text{ \AA}$ , whereas the width in  $\omega$  denotes a mosaic spread of  $1 \text{ mrad}$ .

### Data processing

The raw data consisting of either two-dimensional  $\omega$ - $2\theta$  or three-dimensional  $\omega$ - $\chi$ - $2\theta$  sets were first corrected for instrumental line broadening by deconvolution with a 333 reference reflection from a Si single crystal recorded in the same geometrical arrangement as the titanite crystal. The deconvolution as described in Press et al. (1989) was conducted for each  $\omega$  set to remove the detector broadening in  $2\theta$ . The resulting files consisted of angles-intensity data and were transformed into reciprocal space by calculating the relevant orientation matrices. This procedure is part of a software package that has been developed by us to facilitate the processing of large area detector frames and will be published in a separate paper.

## RESULTS AND DISCUSSION

Intensities, line widths, and Lorentzian fractions were obtained by fitting the temperature-dependent rocking curves of reflections  $\bar{2}16$ ,  $\bar{1}42$ , and  $\bar{1}43$ . As an example, we show the temperature dependent intensity maps as a series of  $\omega$ - $2\theta$  plots for reflection  $\bar{2}16$  in Figure 1. The temperature evolution of the rocking curves in  $\omega$  for reflections  $\bar{2}16$  and  $\bar{1}42$  are depicted in Figure 2a and 2b, respectively. Graphic representations of peak heights and Lorentzian fractions as a function of temperature for reflection  $\bar{2}16$  are given in Figure 3.

### Bragg scattering

At  $T < T_c$  the full width at half maximum values of the peaks in  $\omega$  are of the order of  $0.06^\circ$  (Gaussian) and  $0.15^\circ$  (Lorentzian) and vary little with temperature. The line width  $\delta\theta$  (in rad) of a Bragg peak is related to the size of the diffracting volume  $s$  by means of the Scherrer

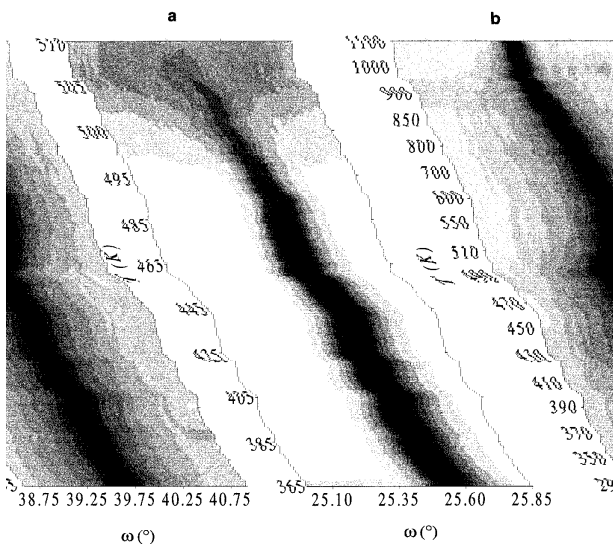


FIGURE 2. Temperature evolution of the rocking-curve profiles of reflections 216 (a) and 142 (b).

equation:  $\delta\theta \approx \lambda_0 s / \cos \theta$ , where  $\lambda_0$  and  $\theta$  are the wavelength and the diffraction angle, respectively. Using this formula, for a width of 2.5 mrad we obtain a domain size of at least 1000 Å (Fig. 1, diagonal direction along streak). Similarly, the rocking-curve width  $\delta\theta \approx 1$  mrad yields the mosaic spread. Even if one concedes some coherent scattering from multiple domains this length scale is much longer than that obtained by electron microscopy at temperatures below  $T_c$  on a different sample (Van Heurck et al. 1991). The electron-microscopic observation must be taken with some caution, however, because Van Heurck et al. (1991) also reported a possible effect of the sample size on the characteristic length scale of the microstructure. These authors found a coarser microstructure in a thicker sample. It is not clear to us whether the fine microstructure seen by them is a consequence of the fact that thin samples were used for transmission electron microscopy or whether impurities were present in their samples. The latter case may be indicated by the fact that the same authors observed other samples without anti-phase boundaries (Van Tendeloo, personal communication) in the same way that our synthetic crystal showed almost no APBs.

We now describe the temperature dependence of the profiles of two superstructure reflections (Figs. 3 and 4). The disappearance of superstructure reflections  $hkl$  with  $k + l$  odd indicates the transformation to an  $A$ -centered lattice. However, the overall intensities of these reflections, which should be extinct in  $A2/a$ , show remaining diffuse scattering above  $T_c$ . Only the Bragg intensities (Gaussian part of the profiles) fall rapidly with increasing temperature and disappear completely at  $T_c$ . We correlate the Gaussian height of the rocking curve with the square of an appropriate long-range order parameter  $Q$ :

$$I \propto Q^2 \propto |T - T_c|^{2\beta} \leftrightarrow \ln(\sqrt{I}) \propto \beta \ln(|T - T_c|)$$

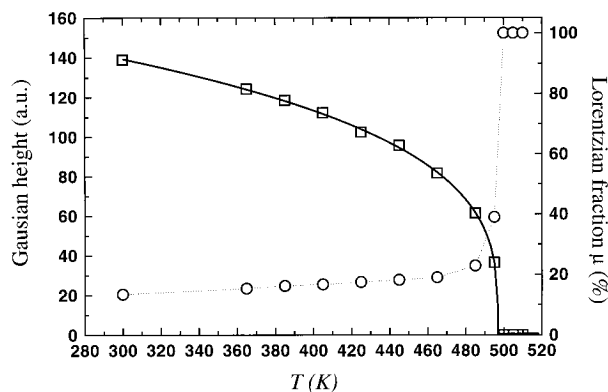


FIGURE 3. Temperature dependence of the Gaussian heights (squares) and Lorentzian fractions  $\mu$  (circles) of reflection 216. The solid line is the fit to the heights ( $\propto Q^2$ ) yielding  $\beta = 0.146(3)$  and  $T_c = 497.0(4)$  K.

where  $\beta$  is the effective order parameter exponent and  $T_c$  is the transition temperature for a continuous structural phase transformation. The Gaussian heights are fitted by this function with  $T_c = 497(1)$  K and  $\beta = 0.146(3)$  for reflection 216 and  $\beta = 0.15(1)$  for 143, respectively (Fig. 4). These  $\beta$  values are equal to the ones obtained in earlier optical and X-ray work (Bismayer et al. 1992; Schmidt et al. 1993) and similar to the value  $\beta = 0.13$  measured using Raman spectroscopy (Salje et al. 1993).

The variation of the long-range order parameter measured by X-ray diffraction, which averages over comparatively large sample volumes, is usually obscured by additional diffuse scattering from isolated ordered domains in the high-temperature form. Here we have shown that the true thermodynamic behavior of the order parameter is obtained by separating Bragg and diffuse scattering from the superstructure reflections. The Gaussian heights

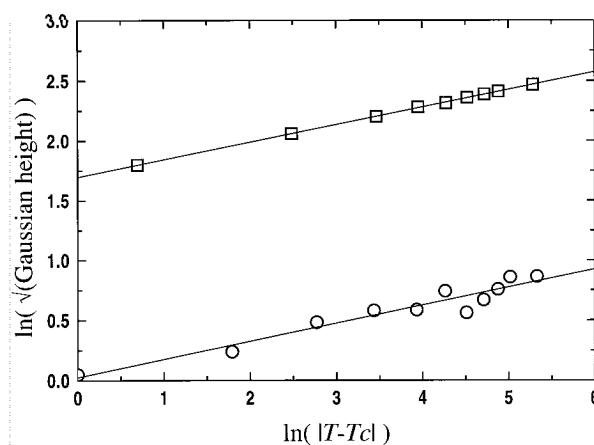


FIGURE 4. Double logarithmic plot of the square root of the Bragg intensity (Gaussian component) vs. the reduced temperature  $|T - T_c|$  of reflections 216 (squares) and 143 (circles). The solid lines are linear fits to the data; the slope is the order parameter exponent  $\beta$ .

of the rocking curves follow the behavior of  $Q^2$  proving that we indeed observe a true phase transition with well-defined long-range ordering. There is no observable long-range order in our sample at  $T \geq T_c$ , and any transition mechanism for titanite involving non-convergent ordering or the existence of intrinsic conjugated fields can be ruled out on the basis of these results.

### Diffuse scattering

The Lorentzian contribution to the  $\bar{2}16$  rocking curve is of the order of  $\sim 20\%$  for temperatures below  $T_c - 20$  K. The characteristic mosaic spread of  $\omega$  corresponds to a length of  $800 \text{ \AA}$ , whereas the diffuse elongation in the  $\omega$ - $2\theta$  plane leads to a length of  $\sim 500 \text{ \AA}$ . These lengths do not increase with increasing temperature as would be expected for the correlation length of the phase transition. Instead we observed a further broadening of the diffuse reflection (i.e., a decrease of the equivalent length scale) on heating up to  $510 \text{ K}$ . At even higher temperatures the diffuse intensity was too much spread out in reciprocal space to be detected as a well-defined diffraction signal. The diffuse scattering may well be correlated with the appearance of precursor short-range order with APBs between ordered and anti-ordered domains. In such a model the size of the domains (including possibly wide APBs) decreases to less than  $200 \text{ \AA}$  at  $T_c$ . At higher temperatures the characteristic length scale becomes even smaller, and the notion of "domains" becomes meaningless. Our experiments show clearly no indication of Bragg scattering of symmetry forbidden reflections at  $T > T_c$ .

### Phase transition(s) at higher temperatures

Spectroscopic investigations (Zhang et al. 1995, 1996; Meyer et al. 1996) have revealed that titanite shows a second phase transition at  $825 \text{ K}$ . As the exact space groups of the various phases are still not known (except for the room temperature phase:  $P2_1/a$ ), we tentatively denote the room temperature phase  $\alpha$ . As discussed above, the  $\alpha$  phase transforms into the  $\beta$  phase at  $497 \text{ K}$  by means of continuous phase transition. It then transforms into the  $\gamma$  phase at  $825 \text{ K}$ . The transition  $\beta \leftrightarrow \gamma$  follows classic second-order behavior (Zhang et al. 1996). We now report additional evidence for this transition and discuss the possibility of a further phase transformation,  $\gamma \leftrightarrow \delta$ , near  $1150 \text{ K}$ .

In our measurements, the position of the maximum of the rocking curve in Figure 2b (reflection  $\bar{1}42$ ) shows an anomaly at the  $\beta \leftrightarrow \gamma$  transition. Furthermore, the  $2\theta$  angle of  $\bar{1}42$  and its Bragg intensity also clearly shows the phase transitions  $\alpha \leftrightarrow \beta$  and  $\beta \leftrightarrow \gamma$  (Fig. 5). The spontaneous strains of these two phase transitions appear to be of the same absolute value but of opposite sign, i.e., the temperature dependencies of  $2\theta$  in the phases  $\alpha$  and  $\gamma$  are rather similar with little thermal expansion in the  $\beta$  phase. The disappearance of the diffraction intensity of the  $\bar{1}42$  reflection upon heating might indicate another phase transition to a high-temperature phase  $\delta$  at about

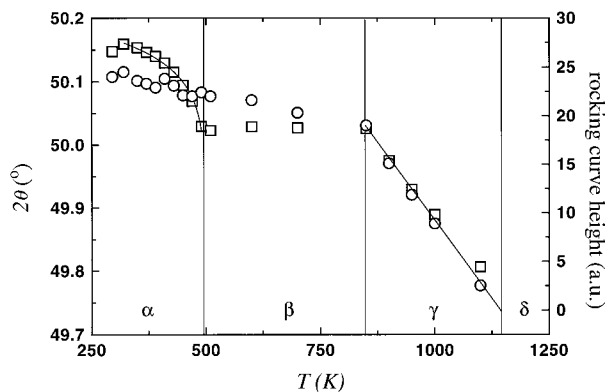


**FIGURE 5.** Temperature dependence of the  $2\theta$  position (squares) of reflection  $\bar{1}42$  and its rocking-curve heights (circles). The phase transitions  $\alpha \leftrightarrow \beta$  and  $\beta \leftrightarrow \gamma$  are correlated with changes of the diffraction angles. The Bragg intensity seems to disappear at  $\sim 1150 \text{ K}$  (solid line), which might indicate another phase transition,  $\gamma \leftrightarrow \delta$ , at this temperature.

$1150 \text{ K}$  (Fig. 5). Further experimental work testing this hypothesis is needed.

### ACKNOWLEDGMENTS

We are indebted to H. Boysen for useful discussions and thank M. Zhang and H. Meyer for making preprints on the second phase transition in titanite available to us. U.B. acknowledges financial support by the DFG. The project was also supported by NERC.

### REFERENCES CITED

- Bismayer, U., Schmahl, W.W., Schmidt, C., and Groat, L.A. (1992) Linear birefringence and X-ray diffraction studies of the structural phase transition in titanite,  $\text{CaTiSiO}_5$ . *Physics and Chemistry of Minerals*, 19, 260–266.
- Chrosch, J. and Salje, E.K.H. (1994) Thin domain walls in  $\text{YBa}_2\text{Cu}_3\text{O}_{7-y}$  and their rocking curves: An X-ray diffraction study. *Physica C*, 225, 111–116.
- (1996) High-resolution X-ray diffraction methods for the structural characterization of crystalline materials. *Ferroelectrics*, 187, 1–10.
- Kek, S., Aroyo, M., Bismayer, U., Meyer, H., Schmidt, C., Eichhorn, K., and Krane, H.G. (1994) Synchrotron radiation study of the crystal structure of titanite,  $\text{CaTiSiO}_5$ , at  $100 \text{ K}$ ,  $295 \text{ K}$ , and  $530 \text{ K}$ : a model for a two-step structural transition. HASYLAB/DESY Annual Report, 453–454.
- Locherer, K.R., Hayward, S.A., Hirst, P.J., Chrosch, J., Yeadon, M., Abell, J.S., and Salje, E.K.H. (1996) X-ray analysis of mesoscopic twin structures. *Philosophical Transactions of the Royal Society (London)* A354, 2815–2845.
- Meyer, H.W., Zhang, M., Bismayer, U., Salje, E.K.H., Schmidt, C., Kek, S., Morgenroth, W., and Bleser, T. (1996) Phase transformation of natural titanite: an infrared, Raman spectroscopic, optical birefringence, and X-ray diffraction study. *Phase Transitions*, 59, 39–60.
- Press, W.H., Flannery, B.P., Teukolsky, S.A., and Vetterling, W.T. (1989) *Numerical recipes in Pascal*, p. 454. Cambridge University Press, Cambridge.
- Salje, E.K.H. (1995) A novel 7-circle diffractometer for the rapid analysis of extended defects in thin films, single crystals and ceramics. *Phase Transitions*, 55, 37–56.
- Salje, E.K.H. and Chrosch, J. (1996) X-ray diffraction analysis of twin walls in ferroelastic  $\text{YBa}_2\text{Cu}_3\text{O}_{7-\delta}$ . *Ferroelectrics*, 183, 85–94.
- Salje, E.K.H., Schmidt, C., and Bismayer, U. (1993) Structural phase transition in titanite,  $\text{CaTiSiO}_5$ : A Raman spectroscopic study. *Physics and Chemistry of Minerals*, 19, 502–506.
- Schmidt, C., Bismayer, U., Riedel, D., Kek, S., and Eichhorn, K. (1993)

- Phase transition and diffuse scattering in synthetic titanite,  $\text{CaTiSiO}_5$ . HASYLAB/DESY Annual Report, 123.
- Speer, J.A. and Gibbs, G.V. (1976) The crystal structure of synthetic titanite,  $\text{CaTiSiO}_5$ , and the domain textures of natural titanites. *American Mineralogist*, 61, 238–247.
- Taylor, M. and Brown, G.E. (1976) High-temperature structural study of the  $P2_1/a \leftrightarrow A2/a$  phase transition in synthetic titanite,  $\text{CaTiSiO}_5$ . *American Mineralogist*, 61, 435–447.
- Van Heurck, C., Van Tendeloo, G., Ghose, S., and Amelinckx, S. (1991) Paraelectric- antiferroelectric phase transition in titanite,  $\text{CaTiSiO}_5$ . II. Electron diffraction microscopic studies of the transition dynamics. *Physics and Chemistry of Minerals*, 17, 604–610.
- Wruck, B., Salje, E.K.H., Zhang, M., Abraham, T., and Bismayer, U. (1994) On the thickness of ferroelastic twin wall in lead phosphate  $\text{Pb}_3(\text{PO}_4)_2$ : An X-ray diffraction study. *Phase Transitions*, 48, 135–148.
- Zhang, M., Salje, E.K.H., Bismayer, U., Unruh, H.-G., Wruck, B., and Schmidt, C. (1995) Phase transition(s) in Titanite  $\text{CaTiSiO}_5$ : An infrared spectroscopic, dielectric response and heat capacity study. *Physics and Chemistry of Minerals*, 22, 41–49.
- Zhang, M., Salje, E.K.H., and Bismayer, U. (1997) Structural phase transition near 825 K in titanite: Evidence from infrared spectroscopic observation. *American Mineralogist*, 82, 30–35.

MANUSCRIPT RECEIVED OCTOBER 7, 1996

MANUSCRIPT ACCEPTED MARCH 13, 1997